RSC Advances

ROYAL SOCIETY OF CHEMISTRY

www.rsc.org/advances

Investigation on Aggregation Behavior of Photo-Responsive System Composed of *1*-Hexadecyl-*3*-methylimidazolium Bromide and *2*-Methoxycinnamic Acid

Mingyong Du, Caili Dai,* Ang Chen, Xuepeng Wu, Yuyang Li, Yifei Liu, Weitao Li, Mingwei Zhao*

School of Petroleum Engineering, China University of Petroleum (East China), Qingdao, Shandong, 266580, P. R. China

* Caili Dai Email: daicl@upc.edu.cn
Tel: +86-532-86981183 Fax: +86-532-86981161
* Mingwei Zhao Email: zhaomingwei@upc.edu.cn
Tel: +86-532-86981183 Fax: +86-532-86981161

Abstract

A novel fluid system composed of *2*-methoxycinnamic acid (*trans*-OMCA) and *1*-hexadecyl-*3*-methylimidazolium bromide (C_{16}mimBr) in aqueous solution was investigated. The compounds *trans*-OMCA and C_{16}mimBr in aqueous solution can self-assemble and form viscoelastic wormlike micelles. Concentration of *trans*-OMCA and C_{16}mimBr has significant influence on its rheological properties. The samples were characterized by rheological measurements. Structural isomerization of *trans*-to-*cis* of *trans*-OMCA would come into existence after UV light irradiation. Transformation of the system after UV light irradiation was determined by UV-vis absorption spectra, rheological measurement and cryo-TEM observation. Surface tension measurements were carried out to investigate the role of trans-OMCA and UV light of C_{16}mimBr aqueous solution. Critical aggregation concentration (*cac*), effectiveness of surface tension reduction (Π_{cac}), maximum excess surface concentration (Γ_{max}) and minimum area occupied per surfactant molecule (a_s) were obtained. Critical packing parameter was introduced to express the mechanism of aggregation behavior transition.

Keywords: wormlike micelles; rheological property; isomerization; UV light irradiation, surface tension, critical packing parameter

1. Introduction

Surfactants could aggregate into highly organized structures, for example, micelles, fibers, vesicles, and lamellar phases.[1-4] As one of the most important structures, wormlike micelles have received considerable attention because of their particular micellar structures and unique rheological response.[5-9] These micelles with flexible and elongated characters can easily entangle into a dynamic reversible network structure. The structures can break and reform, in this way, they are usually called "living" or "equilibrium" polymers.[10-12] Wormlike micelles have extensive application fields and offer great potential in numerous aspects because of their fascinating properties, for example, rheology control, drag reduction agent, heat transfer, drug delivery, and enhanced oil recovery.[13-15]

Scientists have already focused on craft adaptable materials inspired by nature.[16-18] The structure or functionality of these materials can dynamically alter once stimulated by these factors, for example, light, temperature, electric, and pH.[19-27] Among these systems formed by the environment stimulated materials, smart wormlike micelles are a particular area of highly promising development.[28] The smart wormlike systems usually rely on small amphiphilic molecules and their self-assembly. The structural change may lead to macroscopic characteristics variations, such as viscosity and elasticity. Smart wormlike micelles have attracted considerable interest due to their promising characteristics, and have many technological application.[27,29-31] Compared with other factors, such as pH, salinity, redox reagent, and temperature, light plays a vital important role and have a set of significant advantages.[32-34] This can be operated in a clean environment without any other additional chemicals, avoiding any changes of thermodynamic conditions. Besides, light is a reliable and cheap energy resource, and can be performed at an accurate distance, which is precious in research field, such as nanoscience, nanotechnology, and medical application.[35,36]

Therefore, light has always been used as a stimuli by exploiting *trans*-to-*cis* isomerization in wormlike micelles.[34,37-40] The investigation of light-responsive wormlike micelles was first reported in 1980s.[41,42] There are mainly two ways forming

light-responsive wormlike micelles: adding certain light-sensitive additives into surface active ionic liquid solutions or introducing functional groups into the molecules.[27,43-45] Light-responsive wormlike micelles always take advantage of some light-induced *trans*-to-*cis* isomerization of additives containing certain functional groups or surfactants.[46,47] Obviously, these changes could affect the aggregation behavior of the molecules inside the aggregates, thus properties of wormlike micelles would alter either.

In this paper, we studied the aggregation behavior of *2*-methoxycinnamic acid (*trans*-OMCA) and *1*-hexadecyl-*3*-methylimidazolium bromide (C_{16}mimBr) in aqueous solution, and transition of micelles induced by UV irradiation was observed. Structures of C_{16}mimBr and *trans*-OMCA were shown in Scheme 1. We just want to construct a photo-responsive system with the help of the surfactant and the photo-isomerized molecule. In the present work, the system is composed of C_{16}mimBr and *trans*-OMCA, which contains aromatic rings in their molecules. The complex interactions exist in the system, such as electrostatic interactions, hydrophobic interactions and π-π stacking interactions, which may result in the rich phase behaviors. This inspires us to do this work. We expect that this work will help to better understand the photo-responsive system and expand their application.

2. Experimental section

2.1 Materials.

The compounds *1*-methylimidazole (99%), *1*-bromohexadecane (97%), dichloromethane (99.5%), tetrahydrofuran (THF) (99%), and *2*-methoxycinnamic acid (*trans*-OMCA) (98%) were purchased from Aladdin Chemical Reagent Co., Ltd. (Shanghai, China). Ultrapure deionized water was made from Eree water purification systems. Solutions contain *trans*-OMCA were prepared with a slight excess of base (NaOH).

Synthesis of *1*-hexadecyl-*3*-methylimidazolium bromide (C_{16}mimBr)

C_{16}mimBr was synthesized according to a paper published before.[48] The solution of *1*-bromohexadecane in dichloromethane was added to *1*-methylimidazole dissolved in dichloromethane. The mixture was stirred under a nitrogen atmosphere for 48 hours at

75–80 ℃. Then the product was cooled to room temperature and dichloromethane was evaporated. The product was recrystallized from THF at least three times and dried under vacuum for 48 hours at 50 ℃. The product was characterized by ^{1}H-NMR spectroscopy (400 MHz) using D_2O as solvent. The ^{1}H-NMR result is recorded as following:

C_{16}mimBr δ_H: 9.03 (s, 1H), 7.37 (t, 2H), 4.00 (t, 2H), 3.72 (s, 3H), 1.68 (s, 2H), 1.13 (m, 26H), 0.61 (t, 3H).

2.2 Characterization

UV irradiation

Samples were irradiated by a CHF-XM500-500W ultrahigh pressure short arc mercury lamp with a 365nm filter for two hours. The experiment was carried out in a water bath of 25 ℃ under stirring.

UV-vis spectroscopy measurement

The UV-vis spectroscopy measurements of the samples before and after UV irradiation were employed on a UNIC-2802 UV-vis spectrophotometer at room temperature. In this section, water was used as the solution.

Rheology measurements

An AR2000 rheometer (TA Instruments, New Castle, DE) was employed to investigate rheology properties of the samples. Samples were run on a cone and plate geometry (40mm diameter, 2° cone angle). Dynamic frequency sweep measurement was conducted in the linear viscoelastic region. The region was determined from the dynamic strain sweep measurement. The shearing rate ranges from 0.001 to 1000s-1. The zero-shear viscosity (η_0) was obtained from viscosity curve to the vertical coordinates. All experiments were conducted at 25 ℃.

Cryo-TEM

Loading 5μL solution onto a TEM carbon grid using a micropipette. The TEM carbon grid was blotted with two pieces of filter paper in order to form a thin film suspended on the mesh hole. About 5 seconds later, samples were plunged into a reservoir of liquid

enhance at -165 ℃. The samples were stored in liquid nitrogen till they were transferred to a cryogenic sample holder (Gatan 626) and examined with a JEOL JEM-1400 TEM (120KV) at -174 ℃. The phase contrast was enhanced by underforce. Images were recorded on a Gatanmultiscan CCD and processed with a Digital Micrograph. The cryo-TEM observations were performed in China University of Petroleum (Eastern China).

Surface tension measurements

Surface tension measurements were carried out by a model JYW-200B surface tensiometer (Chengde Dahua Testing Instrument Co., Ltd. Hebei, China). The temperature was kept at 25 ℃ with the help of a thermostatic bath. Surface tension was measured through a ring method and all tests were repeated at least twice until the results were repeatable.

3. Results and discussion

3.1 Phase behavior of C_{16}mimBr/*trans*-OMCA system

In order to investigate the phase behavior of C_{16}mimBr/*trans*-OMCA system, different amounts of *trans*-OMCA were added into a series of C_{16}mimBr solutions with a constant concentration. Figure 1 shows the phase diagram of C_{16}mimBr/*trans*-OMCA system at 25 ℃. Phase I and phase II are divided by a solid line, these regions behave different aggregation behaviors. Just as shown in this figure, samples in phase I are clear and transparent with no viscoelasticity. Specifically, when C_{16}mimBr concentration is lower than 80 mM, the liquid is no viscoelasticity liquid even the concentration of *trans*-OMCA is up to 100 mM. However, with the addition of *trans*-OMCA in certain C_{16}mimBr aqueous solutions, changes can be observed, and the sample turns into high viscoelastic solution. Just as the figure shown, the fluid in the bottle cannot flow even the bottle was inverted. It is predicted that wormlike micelles are formed in this region, which will be proved in the following sections.

3.2 Rheological properties of *trans*-OMCA and C_{16}mimBr system

3.2.1 Effect of trans-OMCA concentration on rheology properties

In order to investigate the effect of *trans*-OMCA concentration on the micelle formation

of C_{16}mimBr/*trans*-OMCA system at 25 ℃, samples were prepared by adding different amount of *trans*-OMCA to a fixed C_{16}mimBr solution (150 mM). Figure 2a shows the steady-shear rate viscosity curves of these systems. The viscosity of the system is very low and displays a Newtonian behavior [49,50] under low *trans*-OMCA concentrations. However, changes appear when certain amount of *trans*-OMCA is added. The fluid exhibits high viscosity at low shear rates and the solution displays a Newtonian property. Nevertheless, viscosity falls while the shear rate raises, and shear-thinning behavior presents. High viscosity in the Newtonian plateau can be attributed to the presents of entangled networks of wormlike micelles and perhaps this is a symbol of long wormlike micelles, which will be studied in the following section. Many reports have shown that the entangled network is aligned as the shear rate increases.[51] But the fluid cannot reach an equilibrium condition above a critical shear rate and viscosity falls at this time.

Zero-shear viscosity (η_0) can be obtained according to Carreau model[50], and it is the value of viscosity at the plateau in Figure 2a. Figure 2b presents the curve of η_0 against *trans*-OMCA concentration for this system. In this figure we can tell that η_0 increases with *trans*-OMCA concentration and reaches a peak, then decreases. This phenomenon is similar to the behavior of some ionic surfactant and salt aqueous systems.[52] The increase of η_0 may be a symbol of micellar length growth. Addition of *trans*-OMCA can stimulate the electrostatic repulsions among the headgroups of the surfactant molecules. Consequently, the micellar length increases and micelles begin to overlap and entangled network formed. It has been considered that the decrease of η_0 is a result of branched wormlike micelles.[53] The branched structures tend to slide along the micelles and thus the viscosity will reduce.

Viscoelastic properties of the wormlike micellar samples were studied by frequency sweep measurement. The dynamic rheological behavior for the C_{16}mimBr/*trans*-OMCA system was carried out as a function of *trans*-OMCA concentration at a certain C_{16}mimBr concentration, which is shown in Figure 3a. The lines show relationship of elastic modulus (G') and viscous modulus (G'') *versus* oscillation frequency (ω). At low ω, G' is smaller than G" and the sample shows viscous behavior. Elastic behavior presents at high ω, G' is higher than G'' and G' shows a plateau value at that time. The

samples show viscoelastic property, which indicates the formation of rigid network of entangled wormlike micelles. A crossover point existed according to the lines, the crossover frequency is called ω_{co} and the crossover modulus corresponds to G_{co}. Just as Figure 5a shows, ω_{co} moves backward and then forward as *trans*-OMCA concentration increase from 40 mM to 60 mM. A higher ω_{co} value means poorer viscoelastic behavior. The values of G' and G" are fitted as equation (1) and equation (2) below.[54]

$$G' = G_0 \frac{(\omega\tau)^2}{[1+(\omega\tau)^2]} \quad (1)$$

$$G'' = G_0 \frac{\omega\tau}{[1+(\omega\tau)^2]} \quad (2)$$

Where G_0 stands for the plateau value of shear modulus and τ stands for the stress relaxation time. G_0 and τ can be calculated from equation (3) and equation (4).

$$G_0 = 2G_{co} \quad (3)$$

$$\tau = \frac{1}{\omega_{co}} \quad (4)$$

To better show whether the Maxwell model fits the data, Cole-Cole plots are commonly investigated. The Cole-Cole plot is a curve of G" as a function of G'. It can be obtained from equation (5).

$$G'' + \left(G' - \frac{G_0}{2}\right)^2 = \left(\frac{G_0}{2}\right)^2 \quad (5)$$

The Cole-Cole plots are shown in Figure 3b. It can be seen clearly that at low frequency, all the experimental points follow the Maxwell fluid, which means that the solution behaves as an ideal Maxwell material within the lower shear frequency range. It is a proof that wormlike micelles are formed in this situation. However, when *trans*-OMCA concentration is lower than 30 mM, the system has no viscoelastic response.

3.2.2 Effect of surfactant concentration on rheology property

It can be seen clearly that concentration of *trans*-OMCA has great influence on the viscosity of C_{16}mimBr/*trans*-OMCA system. The impact of surfactant (C_{16}mimBr) concentration on this system is studied. The steady state curves for different surfactant concentration solutions are shown in Figure 4a. It can be seen from the figure that

samples are Newtonian fluids at low concentrations, the viscosity of which is low and could not be affected by the shear rate. However, when C_{16}mimBr concentration is higher than 80 mM, these samples are non-Newtonian fluids and exhibiting a high constant viscosity at low shear rate and shear thinning behavior at high shear rates, which is a typical symbol of wormlike micelles.[55] Figure 4b shows the curve of η_0 obtained from Figure 4a. According to this figure, the value of η_0 increases with the addition of C_{16}mimBr. Low viscosity at low C_{16}mimBr concentrations represents spherical or short rodlike micelles and the addition of C_{16}mimBr may favor the growth of micelles.[56]

3.3 UV-vis light irradiation effect on C_{16}mimBr/*trans*-OMCA system

3.3.1 UV-vis absorption spectra of C_{16}mimBr/trans-OMCA system induced by UV irradiation

Molecules of *trans*-OMCA and *cis*-OMCA obtain different wavelength absorptions in ultraviolet region, the structural transition can be detected by UV-vis spectra. In this way, absorbance spectra of *trans*-OMCA before and after UV-irradiation were obtained to prove the *trans*-to-*cis* transition in Figure 5. Figure 5a shows that, before irradiation, *trans*-OMCA has absorbance peaks at 269 and 312nm. However, UV light irradiation results to blue shifts to 255 and 292nm, significant reduction of the intensity is also presented. As shown in published papers, *cis*-isomer has higher steric hindrance and lower conjugation degree, indicating that the maximum absorption wavelength and the value of intensity are lower than that of *trans*-isomer.[27] This blue shift is a proof of *trans*-to-*cis* transition. Besides, the UV irradiated sample was irradiated by visible light for 24 hours, there is no change in the absorbance spectra, just the same as the black line in Figure 5a. This phenomenon is in accordance with previous published papers.[42]

3.3.2 Rheological properties of C_{16}mimBr/trans-OMCA system after UV irradiation

Then, we studied the effect of UV light irradiation on the system. After irradiated for 2 hours, the sample changed to flowing fluid with low viscosity from viscoelastic fluid. Figure 6a shows the steady shear rheological curve of a 150 mM C_{16}mimBr and 50 mM

trans-OMCA solution after UV irradiation. It can be found that, the solution is Newtonian fluid. The value of η_0 decreases sharply compared with the value of 150 mM C_{16}mimBr and 50 mM *trans*-OMCA solution before irradiation just shown in Figure 2a. This interesting phenomenon indicates the length of wormlike micelles decreases and they even turn into spherical micelles. Figure 6b shows dynamic rheology of this sample. It can be clearly seen that G”>G’ in all frequency regions without a crossover, and this is a symbol of viscous fluid. We can conclude that UV irradiation could induce the viscoelastic fluid to a thin, viscous one, and the length of wormlike micelles may decreases, which could be ascribed to the phase transition from wormlike micelles to rodlike or spherical micelles.

3.3.3 Cryo-TEM investigation on C_{16}mimBr/trans-OMCA system

Cryo-TEM technique was further employed to confirm the effect of UV irradiation for this system. Cryo-TEM images before and after 120 min of UV irradiation are shown in Figure 7. As shown in Figure 7a, a typical wormlike micelle network could be observed, and the network is formed by numerous of wormlike micelles. After UV irradiation, just as Figure 7b shows, wormlike micellar structures are damaged and cannot be detected anymore. The change of wormlike micelles structure could be attributed to the *trans*-to-*cis* isomerization induced by UV irradiation. This phenomenon is in accordance with the rheological results of the *trans*-OMCA (50 mM) + C_{16}mimBr (150 mM) before and after UV irradiation.

3.3.4 Surface tension measurements

Surface tension measurements were carried out to evaluate the aggregation behavior of the aqueous solutions. Aqueous solution of *trans*-OMCA was irradiated by UV light for 120 min before the experiment and it turned into *cis* form. Figure 8 shows the surface tension (γ) of C_{16}mimBr aqueous solution, C_{16}mimBr/*trans*-OMCA aqueous solution and the C_{16}mimBr/*cis*-OMCA aqueous solution. All experiments were carried out at 25 ℃. We can tell that surface tensions of all the three solutions decrease with the addition of surfactant before reaching a plateau at certain C_{16}mimBr concentrations. The critical aggregation concentration (*cac*) obtained from this figure are listed in Table

1. The C_{16}mimBr/*trans*-OMCA solution and C_{16}mimBr/*cis*-OMCA solution have lower *cac* values. Both *trans*-OMCA and *cis*-OMCA molecules have opposite charges against surfactant headgroups. They can compress the electric double layer surrounding the micelles and finally reduce the electrostatic repulsion effect among the headgroups. Finally *cac* values decrease. The effectiveness of surface tension reduction (Π_{cac})[5] can be calculated from the following equation:

$$\Pi_{cac} = \gamma_0 - \gamma_{cmc} \quad (6)$$

Where γ_0 is the surface tension of pure solvent and γ_{cac} is the surface tension of the sample at the *cac*. Π_{cac} shows the equilibrium surface tension reduction caused by the introduction of these molecules. The values in Table 1 shows Π_{cac} increases in the order C_{16}mimBr < *cis*-C_{16}mimBr/*trans*-OMCA < C_{16}mimBr/*trans*-OMCA.

The maximum excess surface tension (Γ_{max}) and the minimum area occupied per surfactant molecule (a_s) are introduced to describe the aggregation behavior in aqueous solution clearly.[5] They are obtained from the Gibbs adsorption isotherm:

$$\Gamma_{max} = -\frac{1}{2RT}\left(\frac{d\gamma}{d\ln C}\right)_T \quad (7)$$

$$a_s = \frac{1}{N_A \Gamma_{max}} \times 10^{23} \quad (8)$$

where R is the gas constant (8.314 J mol^{-1} K^{-1}), T is the absolute temperature, N_A is Avogadro's number (6.022×10^{23} mol^{-1}). Just as Table 1 indicates, the C_{16}mimBr/*trans*-OMCA system obtains the highest Γ_{max} value and the lowest a_s value. The C_{16}mimBr headgroups can adsorb the anionic counterion in *trans*-OMCA, which makes the surfactant molecules packing more closely. However, *cis*-OMCA is more hydrophilic than *trans*-OMCA and less molecules are absorbed[27], this is the reason why the C_{16}mimBr/*cis*-OMCA system is different from the C_{16}mimBr/*trans*-OMCA system.

3.4 Mechanism of micelle transition induced by UV irradiation

The mechanism of micelle transition can be explained by the theory of molecular packing parameter.[57]

$$P = \frac{v_0}{a_s l_0} \quad (9)$$

Where v_0 is the hydrocarbon core volume of a surfactant, a_s is the equilibrium area per

molecule at the surfactant-water interface, l_0 is the length of hydrocarbon chain. The value of P means the critical packing parameter, which can be used to determine the shape of micelles. The critical condition for the formation of different micelles are P=1/3, P=1/2, and P=1 respectively. When P<1/3, spherical micelles can be observed; when 1/3<P<1/2, rodlike or wormlike micelles are obtained; when 1/2<P<1, vesicles exists; when $P \approx 1$ planar bilayers are observed; when P>1, inverted micelles are obtained.

In our system, the value of υ_0 and l_0 can be caculated by the experimental fomular introduced by Tanford.[58]

$$\upsilon_0 = 27.4 + 26.9N_c \quad (10)$$

$$l_0 = 1.5 + 1.265N_c \quad (11)$$

Where N_c is the carbon atom number of alkyl chain.

According to fomular (10) and (11), the value of υ_0 and l_0 for C_{16}mimBr are 457.8 Å^3 and 21.7 Å individually. The value of a_s has been calculated and shown in Table 1. As a result, the critical packing parameter can be calculated, and the value is 0.261. It is apparent that spherical micelles can be observed in C_{16}mimBr aqueous solution and no wormlike micelles would appear theoretically, which is in correspondence with the experimental results. We can calculate the value of P for the other two systems and the result are shown in Table 1, they are 0.420 and 0.379 respectively, and in the extent of 1/3 to 1/2, where rodlike micelles and wormlike micelles can be detected. Once introduced, the compensation ion with opposite charge in *trans*-OMCA tends to insert into the spherical micelles, and the surface charges can be shielded because of electrostatic repulsion. This will lead to the reduction of a_s, and the value of P increases at the same time. As a result, wormlike micelles appear with the addition of certain amount of *trans*-OMCA. After UV irradiation, *trans*-OMCA would transform to *cis*-OMCA. As, reported before, *cis*-OMCA is more hydrophobic than t*rans*-OMCA. The different hydrophobicity is attributed to the net dipole moment. The dipoles tend to add up in the *cis*-OMCA, however, they will cancel each other in the *trans*-OMCA.[27] Less *cis*-OMCA could combine with C_{16}mimBr because of the hydrophobic interaction and

steric hindrance. Thus the value of a_s increases and P decreases, therefore, spherical or rodlike micelles will appear after UV irradiation. This process can be clearly seen in Figure 9.

4. Conclusions

In this paper, we have investigated the rheological behavior and UV light influence of C_{16}mimBr/*trans*-OMCA system in aqueous solution. Rheological measurements were used to observe the influence of *trans*-OMCA and C_{16}mimBr concentration. UV-vis absorption spectra, rheological measurement and cryo-TEM observation were carried out to investigate the influence of UV irradiation on the structural change of *trans*-OMCA and the micelle transition from wormlike micelles to spherical or rodlike micelles. Surface tension measurements were employed to investigate the effect of *trans*-OMCA and UV light irradiation on the micelle formation process. Critical packing parameter theory was used to discover the mechanism of micelle transition.

Acknowledgements

The work was supported by the National Science Fund for Distinguished Young Scholars (51425406), National Natural Science Foundation of China (51174221).

References

(1) Qiao, Y.; Lin, Y.; Wang, Y.; Li, Z.; Huang, J. Metal-driven viscoelastic wormlike micelle in anionic/zwitterionic surfactant systems and template-directed synthesis of dendritic silver nanostructures. *Langmuir*, **2011**, 27, 1718-1723.

(2) Yakovlev, D. S.; Boek, E. S. Molecular dynamics simulations of mixed cationic/anionic wormlike micelles. *Langmuir*, **2007**, 23, 6588-6597.

(3) Dai, C.; Du, M.; Zhao, M.; You, Q.; Guan, B.; Wang, X.; Liu, P. Study of Micelle Formation by Fluorocarbon Surfactant N-(2-hydroxypropyl) perfluorooctane Amide in Aqueous Solution *J. Phys. Chem. B*, **2013**, 117, 9922-9928.

(4) Hoffmann, H. Fascinating phenomena in surfactant chemistry. Adv. Mater., **1994**, 6, 116-129.

(5) Dai, C.; Du, M.; Liu, Y.; Wang, S.; Zhao, J.; Chen, A.; Peng, D.; Zhao, M. Aggregation Behavior of Long-Chain Piperidinium Ionic Liquids in Ethylammonium Nitrate. *Molecules*, **2014**, 19, 20157-20169.

(6) Afifi, H.; Karlsson, G. r.; Heenan, R. K.; Dreiss, C. A. Solubilization of oils or addition of monoglycerides drives the formation of wormlike micelles with an elliptical cross-section in cholesterol-based surfactants: A study by rheology, SANS, and cryo-TEM. *Langmuir*, **2011**, 27, 7480-7492.

(7) Raghavan, S. R.; Kaler, E. W. Highly viscoelastic wormlike micellar solutions formed by cationic surfactants with long unsaturated tails. *Langmuir*, **2001**, 17, 300-306.

(8) Zana, R.; Talmon, Y. Dependence of aggregate morphology on structure of dimeric surfactants. *Nature*, **1993**, 362, 228-230.

(9) Han, Y.; Feng, Y.; Sun, H.; Li, Z.; Han, Y.; Wang, H. Wormlike micelles formed by sodium erucate in the presence of a tetraalkylammonium hydrotrope. *J. Phys. Chem. B*, **2011**, 115, 6893-6902.

(10) Won, Y.-Y.; Davis, H. T.; Bates, F. S. Giant wormlike rubber micelles. *Science*, **1999**, 283, 960-963.

(11) Cates, M. Reptation of living polymers: dynamics of entangled polymers in the presence of reversible chain-scission reactions. *Macromolecules*, **1987**, 20, 2289-2296.

(12) Rehage, H.; Hoffmann, H. Viscoelastic surfactant solutions: model systems for

rheological research. *Mol. Phys.*, **1991**, 74, 933-973.

(13) Qi, Y.; Zakin, J. L. Chemical and rheological characterization of drag-reducing cationic surfactant systems. *Ind. Eng. Chem. Res.*, **2002**, 41, 6326-6336.

(14) Stukan, M. R.; Boek, E. S.; Padding, J. T.; Briels, W. J.; Crawshaw, J. P. Flow of wormlike micelles in an expansion-contraction geometry. *Soft Matter*, **2008**, 4, 870-879.

(15) Ezrahi, S.; Tuval, E.; Aserin, A. Properties, main applications and perspectives of worm micelles. *Adv. Colloid Interface Sci.*, **2006**, 128, 77-102.

(16) Lehn, J.-M. Toward self-organization and complex matter r. *Science*, **2002**, 295, 2400-2403.

(17) Fuhrhop, J. H.; Helfrich, W. Fluid and solid fibers made of lipid molecular bilayers. *Chem. Rev.*, **1993**, 93, 1565-1582.

(18) Svenson, S. Controlling surfactant self-assembly. *Curr. Opin. Colloid. In.*, **2004**, 9, 201-212.

(19) Johnsson, M.; Wagenaar, A.; Engberts, J. B. Sugar-based gemini surfactant with a vesicle-to-micelle transition at acidic pH and a reversible vesicle flocculation near neutral pH. *J. Am. Chem. Soc.*, **2003**, 125, 757-760.

(20) Maeda, H.; Yamamoto, A.; Souda, M.; Kawasaki, H.; Hossain, K. S.; Nemoto, N.; Almgren, M. Effects of protonation on the viscoelastic properties of tetradecyldimethylamine oxide micelles. *J. Phys. Chem. B*, **2001**, 105, 5411-5418.

(21) Hubbard Jr, F. P.; Abbott, N. L. A small angle neutron scattering study of the thicknesses of vesicle bilayers formed from mixtures of alkyl sulfates and cationic

bolaform surfactants. *Soft Matter*, **2008**, 4, 2225-2231.

(22) Hubbard, F. P.; Santonicola, G.; Kaler, E. W.; Abbott, N. L. Small-angle neutron scattering from mixtures of sodium dodecyl sulfate and a cationic, bolaform surfactant containing azobenzene. *Langmuir*, **2005**, 21, 6131-6136.

(23) Majhi, P. R.; Blume, A. Temperature-induced micelle-vesicle transitions in DMPC-SDS and DMPC-DTAB mixtures studied by calorimetry and dynamic light scattering. *J. Phys. Chem. B*, **2002**, 106, 10753-10763.

(24) Ghosh, S.; Irvin, K.; Thayumanavan, S. Tunable disassembly of micelles using a redox trigger. *Langmuir*, **2007**, 23, 7916-7919.

(25) Yan, Y.; Xiong, W.; Li, X.; Lu, T.; Huang, J.; Li, Z.; Fu, H. Molecular packing parameter in bolaamphiphile solutions: adjustment of aggregate morphology by modifying the solution conditions. *J. Phys. Chem. B*, **2007**, 111, 2225-2230.

(26) Chu, Z.; Feng, Y. Thermo-switchable surfactant gel. *Chem. Commun.*, **2011**, 47, 7191-7193.

(27) Ketner, A. M.; Kumar, R.; Davies, T. S.; Elder, P. W.; Raghavan, S. R. A simple class of photorheological fluids: surfactant solutions with viscosity tunable by light. *J. Am. Chem. Soc.*, **2007**, 129, 1553-1559.

(28) Stuart, M. A. C.; Huck, W. T.; Genzer, J.; Müller, M.; Ober, C.; Stamm, M.; Sukhorukov, G. B.; Szleifer, I.; Tsukruk, V. V.; Urban, M. Emerging applications of stimuli-responsive polymer materials. *Nat. Mater.*, **2010**, 9, 101-113.

(29) Bohon, K.; Krause, S. An electrorheological fluid and siloxane gel based electromechanical actuator: working toward an artificial muscle. *J. Polym. Sci., Part B:*

Polym. Phys., **1998**, 36, 1091-1094.

(30)Boek, E.; Jusufi, A.; Löwen, H.; Maitland, G. Molecular design of responsive fluids: molecular dynamics studies of viscoelastic surfactant solutions. *J. Phys.: Condens. Matter*, **2002**, 14, 9413.

(31)Morvan, M., Degre, G., Beaumont, J., Colin, A., Dupuis, G., Zaitoun, A & Al-Sharji, H. H. Viscosifying surfactant technology for heavy oil reservoirs. In SPE Heavy Oil Conference Canada. *SPE*. January, **2012**.

(32)Lin, Y.; Cheng, X.; Qiao, Y.; Yu, C.; Li, Z.; Yan, Y.; Huang, J. Creation of photo-modulated multi-state and multi-scale molecular assemblies via binary-state molecular switch. *Soft Matter*, **2010**, 6, 902-908.

(33)Wang, D.; Dong, R.; Long, P.; Hao, J. Photo-induced phase transition from multilamellar vesicles to wormlike micelles. *Soft Matter*, **2011**, 7, 10713-10719.

(34)Eastoe, J.; Vesperinas, A. Self-assembly of light-sensitive surfactants. Soft Matter 2005, 1, 338-347.

(35)Rasmussen, P. H.; Ramanujam, P.; Hvilsted, S.; Berg, R. H. A remarkably efficient azobenzene peptide for holographic information storage. *J. Am. Chem. Soc.*, **1999**, 121, 4738-4743.

(36)Ikeda, T.; Tsutsumi, O. Optical switching and image storage by means of azobenzene liquid-crystal films. *Science*, **1995**, 268, 1873-1875.

(37)Pei, X.; Zhao, J.; Wei, X. Wormlike micelles formed by mixed cationic and anionic gemini surfactants in aqueous solution *J. Colloid Interface Sci.*, **2011**, 356, 176-181.

(38)Baglioni, P.; Braccalenti, E.; Carretti, E.; Germani, R.; Goracci, L.; Savelli, G.;

Tiecco, M. Surfactant-based photorheological fluids: Effect of the surfactant structure. *Langmuir*, **2009**, 25, 5467-5475.

(39) HY, L.; KK, D.; K, S.; T, C.; SR., R. Reversible Photorheological Fluids Based on Spiropyran-Doped Reverse Micelles. *J. Am. Chem. Soc*. **2011**, 133, 8461-8463.

(40) Dupuy, S.; Crawford, L.; Bühl, M.; Nolan, S. P. The Gold(I)-Catalysed Protodecarboxylation Mechanism. *Chem. Eur*. J. **2015**, 21. 3399-3408.

(41) Müller, N.; Wolff, T.; von Bünau, G. Light-induced viscosity changes of aqueous solutions containing 9-substituted anthracenes solubilized in cetyltrimethylammonium micelles. *J. Photoch.*, **1984**, 24, 37-43.

(42) Chu, Z.; Dreiss, C. A.; Feng, Y. Smart wormlike micelles. *Chem. Soc. Rev.*, **2013**, 42, 7174-7203.

(43) Oh, H.; Javvaji, V.; Yaraghi, N. A.; Abezgauz, L.; Danino, D.; Raghavan, S. R. Light-induced transformation of vesicles to micelles and vesicle-gels to sols. *Soft Matter*. **2013**, 9, 11576-11584.

(44) Akamatsu, M.; FitzGerald, P. A.; Shiina, M.; Misono, T.; Tsuchiya, K.; Sakai, K.; Abe, M.; Warr, G. G.; Sakai, H. Micelle Structure in a Photoresponsive Surfactant with and without Solubilized Ethylbenzene from Small-Angle Neutron Scattering. *J. Phys. Chem. B*, **2015**, 119, 5904-5910.

(45) Oh, H.; Ketner, A. M.; Heymann, R.; Kesselman, E.; Danino, D.; Falvey, D. E.; Raghavan, S. R. A simple route to fluids with photo-switchable viscosities based on a reversible transition between vesicles and wormlike micelles. *Soft Matter*, **2013**, 20, 5025-5033.

(46) Bi, Y.; Wei, H.; Hu, Q.; Xu, W.; Gong, Y.; Yu, L. Wormlike Micelles with Photoresponsive Viscoelastic Behavior Formed by Surface Active Ionic Liquid/Azobenzene Derivative Mixed Solution. *Langmuir*, **2015**, 31, 3789-3798.

(47) Yan, H.; Long, Y.; Song, K.; Tung, C. H.; Zheng, L. Photo-induced transformation from wormlike to spherical micelles based on pyrrolidinium ionic liquids. *Soft Matter*, **2014**, 10, 115-121.

(48) Dupont, J.; Consorti, C. S.; Suarez, P. A.; de Souza, R. F. Preparation of 1 - Butyl - 3 - Methyl Imidazolium - Based Room Temperature Ionic Liquids. *Org. Synth.*, **2003**, 236-236.

(49) Wang, X.; Wang, R.; Zheng, Y.; Sun, L.; Yu, L.; Jiao, J.; Wang, R. Interaction between zwitterionic surface activity ionic liquid and anionic surfactant: Na+-driven wormlike micelles. *J. Phys. Chem. B*, **2013**,117, 1886-1895.

(50) Shrestha, R. G.; Shrestha, L. K.; Aramaki, K. Formation of wormlike micelle in a mixed amino-acid based anionic surfactant and cationic surfactant systems. *J Colloid Interface Sci*, **2007**, 311, 276–284.

(51) Bautista, F.; Soltero, J. F. A.; Mac ás, E. R.; Puig, J. E.; Manero, O. Irreversible Thermodynamics Approach and Modeling of Shear-Banding Flow of Wormlike Micelles. *J. Phys. Chem. B*, **2002**, 106, 13018-13026.

(52) Khatory, A.; Lequeux, F.; Kern, F.; Candau, S. Linear and nonlinear viscoelasticity of semidilute solutions of wormlike micelles at high salt content. *Langmuir*, **1993**, 9, 1456-1464.

(53) Hassan, P. A.; Candau, S. J.; Kern, F.; Manohar, C. Rheology of wormlike micelles

with varying hydrophobicity of the counterion. *Langmuir*, **1998**, 14, 6025-6029.

(54) Dreiss, C. A. Wormlike micelles: where do we stand? Recent developments, linear rheology and scattering techniques. *Soft Matter*, **2007**, 3, 956-970.

(55) Rehage, H.; Hoffmann, H. Rheological properties of viscoelastic surfactant systems. *J. Phys. Chem. B*, **1988**, 92, 4712-4719.

(56) Aswal, V.; Goyal, P.; Thiyagarajan, P. Small-angle neutron-scattering and viscosity studies of CTAB/NaSal viscoelastic micellar solutions. *J. Phys. Chem. B*, **1998**, 102, 2469-2473.

(57) Israelachvili, J. N.; Mitchell, D. J.; Ninham, B. W. Theory of self-assembly of hydrocarbon amphiphiles into micelles and bilayers. *J. Chem. Soc.*, **1976**, *72*, 1525-1568.

(58) Tanford, C. Micelle shape and size. *J. Phys. Chem. B*, **1972**, 76, 3020-3024.

Table Captions:

Table 1: surface properties of C_{16}mimBr, C_{16}mimBr/*trans*-OMCA and C_{16}mimBr/*cis*-OMCA systems at 25 ℃ (*trans*-OMCA and *cis*-OMCA concentration are 50 mM individually)

Scheme Captions

Scheme 1: Chemical structure of C_{16}mimBr (a) and OMCA (b)

Figure Captions:

Figure 1: Phase diagram of C_{16}mimBr and *trans*-OMCA system at 25 ℃

Figure 2: Viscosity measurement as a function of *trans*-OMCA concentration (20-100 mM) at a fixed C_{16}mimBr solution (150mM) at 25 ℃. (a), Viscosity *versus* shear rate curves; (b), Zero-shear viscosity *versus trans*-OMCA concentration

Figure 3: (a) Dynamic frequency sweep for different *trans*-OMCA concentration (40 mM, 50 mM, 60 mM) in a 150 mM C_{16}mimBr solution at 25 ℃; (b) cole-cole plots of this system

Figure 4: (a) Viscosity *versus* shear rate curves measurement as a function of C_{16}mimBr (40-200 mM) concentration at a fixed *trans*-OMCA solution (50mM) at 25 ℃; (b) Zero-shear viscosity *versus trans*-OMCA concentration

Figure 5: UV-vis spectra before and after UV irradiation for 2 hours. (a) *trans*-OMCA (50 mM); (b) *trans*-OMCA (50 mM) + C_{16}mimBr (50 mM). All samples were diluted 100 times before investigation.

Figure 6: Typical rheology results of a 150 mM C_{16}mimBr and 50 mM *trans*-OMCA solution after UV irradiation for 2 hours at 25 ℃: (a) viscosity versus shear rate; (b) dynamic frequency sweep

Figure 7: Cryo-TEM images of (a) 150 mM C_{16}mimBr + 50 mM *trans*-OMCA before UV irradiation and (b) after UV irradiation

Figure 8: Surface tension (γ) of C_{16}mimBr aqueous solution, C_{16}mimBr/*trans*-OMCA (50mM) aqueous solution and the C_{16}mimBr/*cis*-OMCA (50mM) aqueous solution at 25 ℃

Figure 9: Mechanism of the aggregation behavior for the photo-responsive system

Table 1

	cac (mM)	*Γcac* (mN/m)	*Πcmc* (mN/m)	*Γmax* (μmol/m^2)	a_s (Å^2)	*P*
C_{16}mimBr	0.566	38.98	33.05	2.06	80.7	0.261
C_{16}mimBr/*trans*-OMCA	0.010	37.37	34.63	3.31	50.2	0.420
C_{16}mimBr/*cis*-OMCA	0.019	38.60	33.39	2.99	55.6	0.379

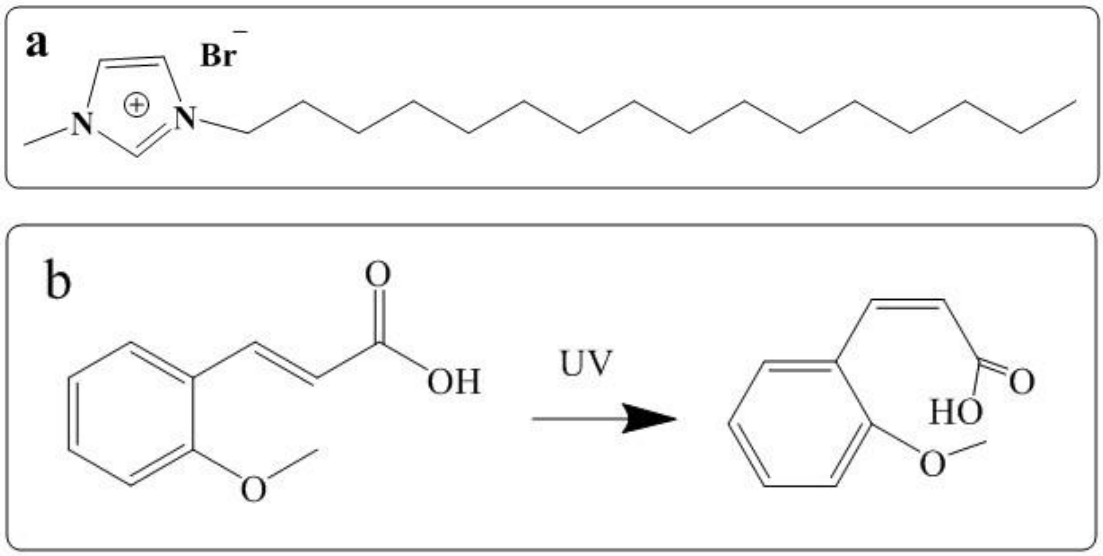

Scheme 1

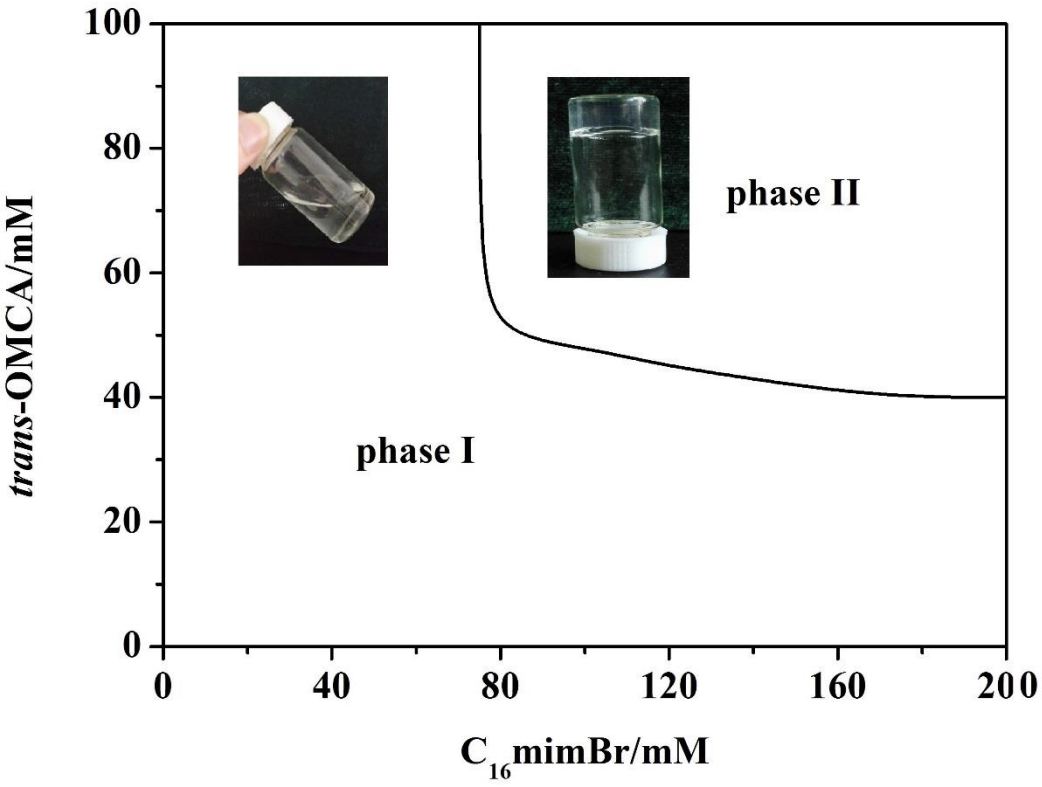

Figure 1

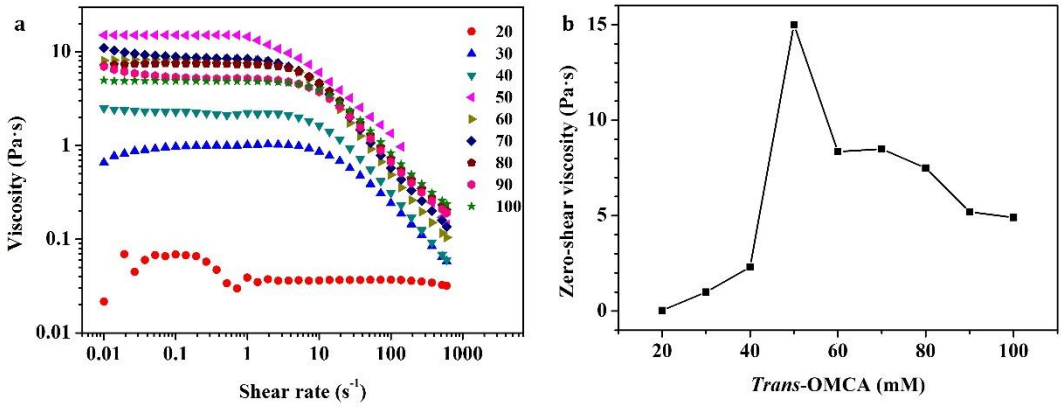

Figure 2

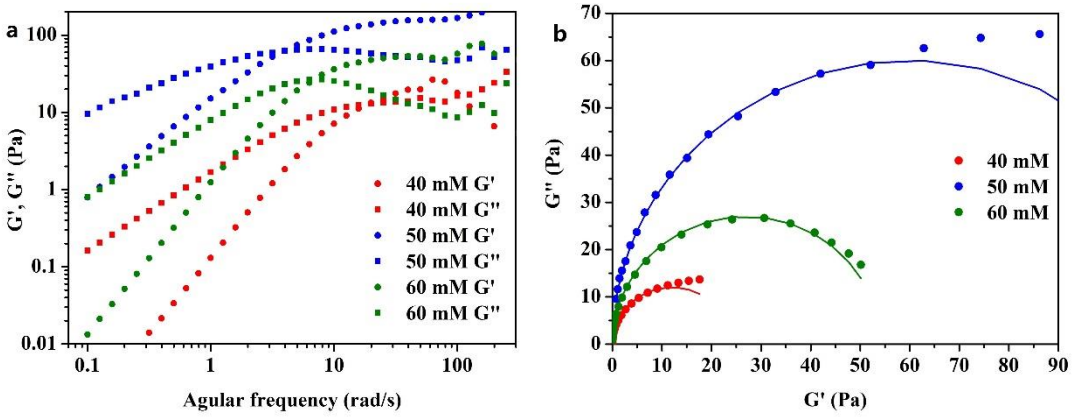

Figure 3

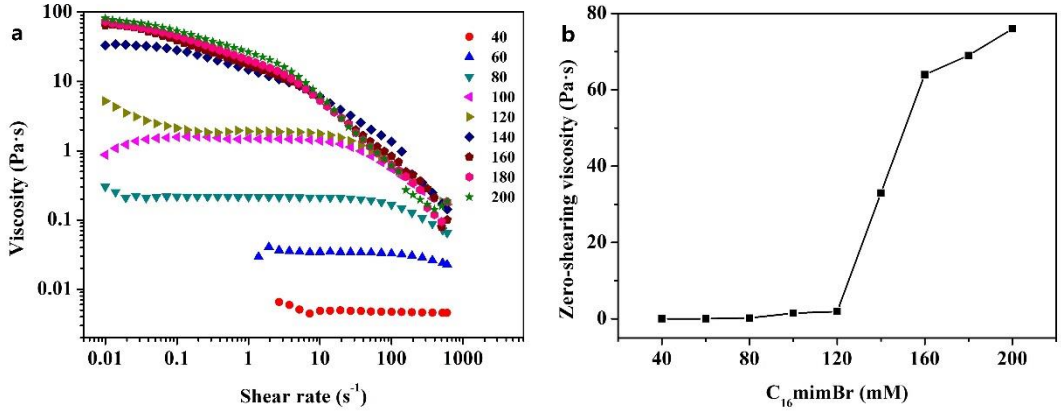

Figure 4

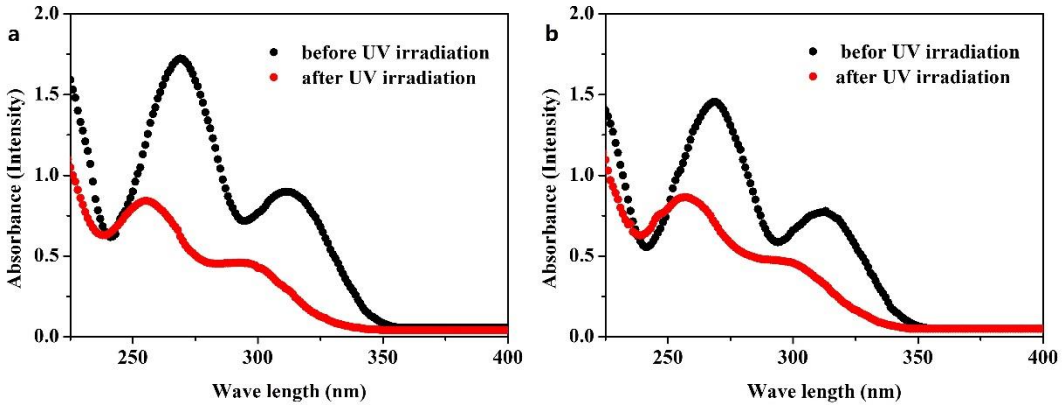

Figure 5

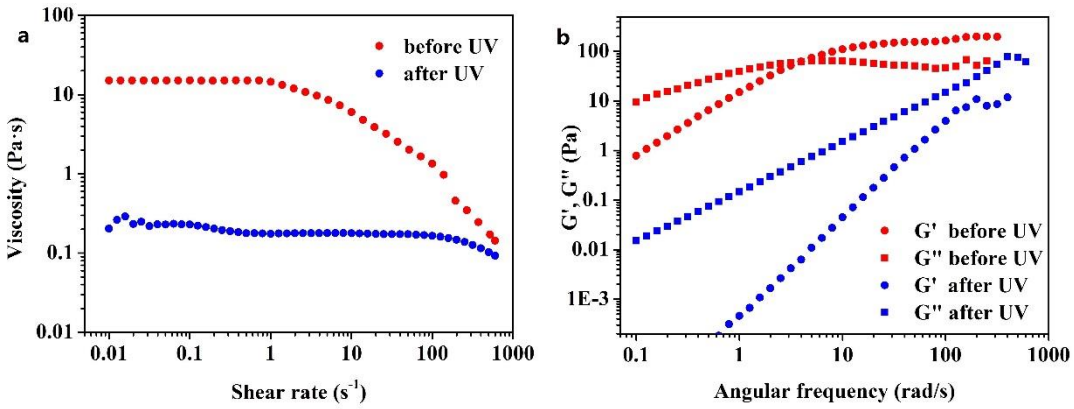

Figure 6

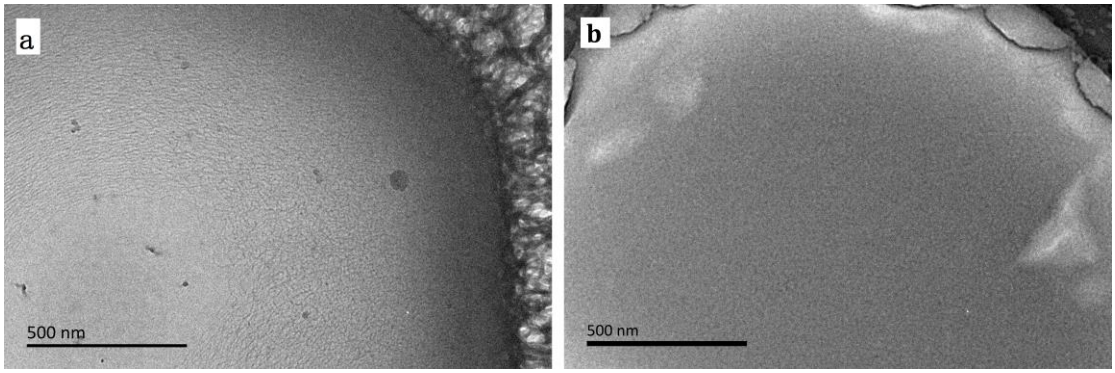

Figure 7

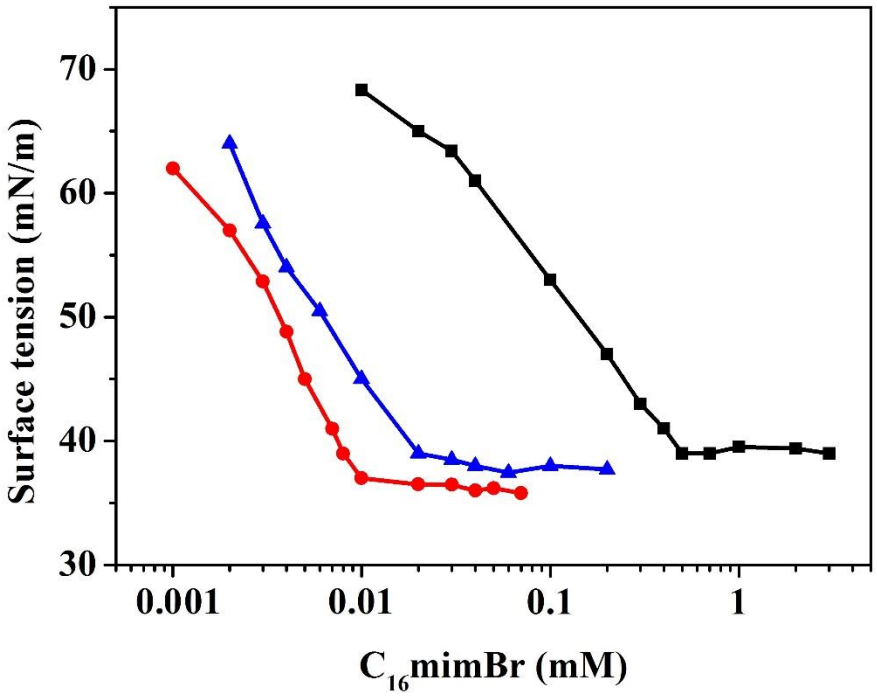

Figure 8

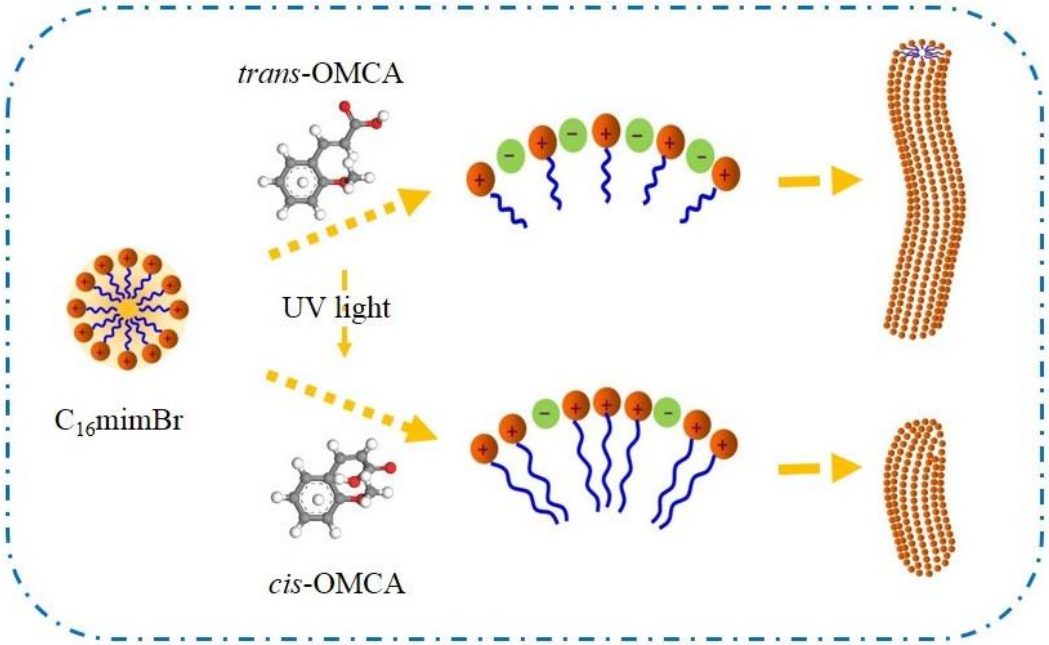

Figure 9